g'_{IA} = set of previously inactive design constraints at X^* that become active at the feasible point X° after disturbances change (i.e., $d = d'$)
$\tilde{g}_{IA}$ = set of previously inactive design constraints at X^* that remain inactive at X° after disturbances change
$\bar{g}_{IA}$ = vector of inequality design constraints which become active at a search point
L = Lagrangian function
m = vector of manipulated variables
$\tilde{m}$ = vector of extrafree manipulated variables
m_D = vector of manipulated variables controlling primary controlled variables
r = regulatory control functions
x = vector of states
$\bar{x}$ = vector of variables composed of x, d, and m_D
$\tilde{x}$ = vector of variables composed of x and m_0.
X° = a feasible operating point
X^* = design optimum

Greek Letters

β = constrained sensitivity of Φ with respect to $\tilde{m}$ at X°
λ = vector of Lagrange multipliers for equality constraints $f(\bar{x}, \tilde{m}) = 0$
λ_A = vector of Kuhn-Tucker multipliers for active design constraints
λ_{IA} = vector of Kuhn-Tucker multipliers for inactive design constraints
Φ = objective function
∇ = gradient operator

LITERATURE CITED

Arkun, Y., "Design of Steady-State Optimizing Control Structures for Chemical Processes," Ph.D. Thesis, Univ. of Minnesota (March, 1979).

Barkelew, C. H., "Modern Process Control—State of the Art in Petroleum Refining," *AIChE Symp.* Ser. 159, **72** (1976).

Baxley R. A., "Local Optimizing Control for Distillation," *Instrumentation Tech.*, 75 (Oct., 1969).

Buckley P. S., *Techniques of Process Control*, J. Wiley & Sons, Inc. (1964).

Davis, T. A., D. E. Griffin, and P. U. Webb, "Cat Cracker Optimization and Control," *Chem. Eng. Prog.*, **70**, No. 11, 53 (Nov., 1974).

DeBrosse C. J., and A. W. Westerberg, "A Feasible-Point Algorithm for Structured Design Systems in Chemical Engineering," *AIChE J.*, **19**, No. 2, 251 (1973a).

Douglas, J. M., "Preliminary Process Design Part III, Quick Estimates of Control Economics," *AIChE Annual Meeting*, New York (1977).

Duyfjes, G., and P. M. E. M. Van Der Grinten, "Application of a Mathematical Model for the Control and Optimization of a Distillation Plant," *Automatica*, **9**, 537 (1973).

Ellingsen, W. R., "Implementation of Advanced Control Systems, *AIChE Symp.* Ser. 159, **72** (1976).

Findeisen, W., "Lectures on Hierarchical Control Systems," Univ. of Minnesota (1976).

Gaines, L. D., and J. L. Gaddy, "Univ. of Missouri-Rolla PROPS Users' Guide," Rolla, MO (1974).

Gould, L. A., L. B. Evans, and H. Kurihara, "Optimal Control of Fluid Catalytic Cracking Processes," *Automatica*, **6**, 695 (1970).

Govind, R., and G. J. Powers, "Control System Synthesis Strategies," *AIChE 82nd National Meeting*, Atlantic City, NJ (1976).

Ishida, C., "An Approach to Optimal Process Plant Operation," Japan-US Joint Seminar, Kyoto Japan (June 23, 1975).

Joseph, B., and C. Brosilow, "Inferential Control of Processes," *AIChE J.*, **24**, 485 (1978).

Kaiser, V. A., J. D. Mahoney, T. M Stout, "An Optimum Approach to Optimization," *ISA*, 3.3-1-66 (Oct., 1966).

Kuehn D. R., and H. Davidson, "Computer Control II. Mathematics of Control," *Chem. Eng. Prog.*, **57**, No. 6, 45 (June, 1961).

Kurihara, H., "Optimal Control of Fluid Catalytic Cracking Processes," ScD Thesis, M.I.T. (1967).

Latour, P. R., "Comments on Assessments and Needs," *AIChE Symp.*, Ser. 159, **72** (1976).

Lee, W., and W. V. Weekman, Jr., "Advanced Control Practice in the Chemical Process Industry: A View from Industry," *AIChE J.*, **22** (1976).

Lefkowitz, I., "Systems Control of Chemical and Related Process Systems," *6th IFAC Congress*, Boston, MA (1975).

Maarleveld, A., and J. E. Rijnsdorp, "Constraint Control on Distillation Columns," *Automatica*, **6**, 51 (1970).

Morari, M., "Studies in the Synthesis of Control Structures of Chemical Processes," Ph.D. Thesis, Univ. of Minnesota (Dec., 1977).

Morari, M., Y. Arkun, and G. Stephanopoulos, "An Integrated Approach to the Synthesis of Process Control Structures," *JACC Proceedings*, Philadelphia, PA (1978).

Pohlenz, J. B., "How Operation Variables Affect Fluid Catalytic Cracking," *Oil Gas J.*, **61** (13), 124 (1963).

Rademaker, O., J. E. Rijnsdorp, and A. Maarleveld, *Dynamics and Control of Continuous Distillation Units*, Elsevier Scientific Publishing Co. (1975).

Rijnsdorp, J. E., "Chemical Process Systems and Automatic Control," *Chem. Eng. Prog.*, **63**, No. 7, 97 (July, 1967).

Shah, M. J., and R. E. Stillman, "Computer Control and Optimization of a Large Methanol Plant," *Ind. and Eng. Chem.*, **62**, No. 12, 59 (Dec., 1970).

Umeda, T., and T. Kuriyama, "A Logical Structure for Process Control System Synthesis," *IFAC Congress*, Helsinki, Finland (1978).

Webb, P. U., B. E. Lutter, and R. L. Hair, "Dynamic Optimization of FCC Units," *AIChE Annual Meeting*, New York (1977).

Weber, R., and C. Brosilow, "The Use of Secondary Measurements to Improve Control," *AIChE J.*, **18**, 614 (1972).

Westerberg, A. W., and C. J. DeBrosse, "An Optimization Algorithm for Structured Design System," *AIChE J.*, **19**, 335 (1973b).

Manuscript received July 23, 1979; revision received April 21, and accepted May 7, 1980.

Analysis of Drop Size Distributions in Lean Liquid-Liquid Dispersions

GANESAN NARSIMHAN
DORAISWAMI RAMKRISHNA
School of Chemical Engineering
Purdue University
West Lafayette, Indiana 47907

JAI P. GUPTA
Department of Chemical Engineering
Indian Institute of Technology
Kanpur, 208016, India

Experimental measurements of transient drop size distributions in a stirred liquid-liquid dispersion (with low dispersed phase fraction) have been used concomitantly with population balance theory to recover the transition probability of droplet breakage, based on a similarity concept. The data remarkably uphold the proposed similarity hypothesis, and the estimated probability function displays the same qualitative trend as the model due to Narsimhan et al. (1979).

SCOPE

The analysis of rate processes in liquid-liquid dispersions (as in other dispersed phase systems) is complicated by their dependence on the dynamics of droplet breakage and coalescence and rate processes occurring in single droplets. The framework of population balances is ideally suited to this task, provided certain essential implements of the analysis are properly identified. These implements are transition probability (or simply rate) functions characterizing random droplet breakage and

Correspondence concerning this paper should be addressed to Doraiswami Ramkrishna.

0001-1541-80-3821-0991-$01.15.

coalescence. In a stirred dispersion, it is difficult to find an appropriate basis on which to obtain expressions for the foregoing functions so that methods must be devised to procure this information from suitable experiments in much the same way as rate constants are obtained from kinetic data on chemical reaction systems. Since the unknowns here are rate functions (for example, of drop size) instead of rate constants, this identification procedure is considerably more complicated. If consideration is restricted to lean dispersions, the effects of coalescence are possibly negligible so that this evolution of drop size distributions in such a system, at least in the early stages of agitation, is a result of breakage only. The advantage of this system is that the identification problem for the transition probability of droplet breakage is linear.

The present work is concerned with calculation of the droplet breakage probability function from experimental data on drop size distributions obtained from a lean liquid-liquid dispersion in a stirred batch vessel. The drop size distributions were obtained by a Coulter counter after the droplets were encapsulated by a surface polycondensation reaction.

A concept of similar breakage is introduced which allows the estimation of the transition probability of droplet breakage and the daughter droplet distribution from the transients of drop volume distribution. A test for consistency with similarity is developed. Experimental data on three different dispersed phases have been subjected to the foregoing similarity test and found to be consistent with the concept. The transition probability of droplet breakage and the moments of the daughter droplet distribution were computed up to a multiplicative constant.

CONCLUSIONS AND SIGNIFICANCE

The proposed similarity transformation is upheld remarkably well by data on drop size distributions obtained from transient, batch experiments with three different dispersed phases under different stirring conditions. The transition probability function for droplet breakage shows a steeper decline as drop size decreases towards a maximum stable value. A simple model for the transition probability due to Narsimhan, Gupta and Ramkrishna (1979) based on the incorporation of a Poisson process for the random arrival of eddies on a droplet surface into Levich's (1962) view of droplet breakage is found to display the same qualitative trend as the probability function computed from the data.

The information in this paper could be a valuable source for analyzing rate processes in liquid-liquid dispersion in situations where dynamic droplet phenomena play an important role.

The mathematical framework for the analysis of transient drop size distributions is provided by population balances. The population balance equation required here is that for a pure breakage system, since the effects of coalescence may be excluded because the dispersion is assumed to be lean. In order that quantitative predictions are possible with the aid of population balances, it is necessary that certain key probability functions which appear in the equation are known or identified by analyzing suitably experimental data on transient drop size distributions. The application envisaged pertains to a stirred mixer, in which dispersed phase initially present as large globules are split up into little droplets and into progressively smaller drops in course of time. Measurements of drop size distributions in such dispersions should, in principle, provide the required information for quantitatively recovering the foregoing key probability functions. The functions that are of interest here are those associated with droplet breakage. Thus, the evolution of drop size distributions is characterized by a transition probability of breakage of droplets and the size distribution of the daughter droplets resulting from breakage of a larger (the parent) droplet. The problem of central interest to this paper is the determination of the above functions, given experimental data on drop size distributions. We refer to this as the inverse problem in the discussion that follows.

THE INVERSE PROBLEM AND SIMILARITY

It is assumed that stirring is sufficient to ensure spatial homogeneity of the drop size distribution. The volume fraction of droplets of volume less than v at time t in a batch agitated lean liquid-liquid dispersion is denoted by $F(v,t)$ which is a cumulative distribution function satisfying the conditions

$$F(v,t) = 0, \ (v \leq 0); \ \lim_{v \to \infty} F(v,t) = 1$$

Breakage may be characterized by the transitional breakage probability $\Gamma(v)$, such that $\Gamma(v) \cdot dt$ represents the probability that a droplet of volume v would break in time interval t, $t+dt$ and the volume fraction of daughter droplets with volume less than v formed from breakage of parent droplet of volume v', represented by the function $G(v,v')$ (Ramkrishna, 1974).

For a batch agitated lean liquid-liquid dispersion, it can be shown that

$$\frac{\partial F(v,t)}{\partial t} = \int_v^\infty \Gamma(v') \, G(v,v') \, dF(v',t) \tag{1}$$

$$= \int_v^\infty \Gamma(v') \, G(v,v') \, f(v',t) dv' \tag{1a}$$

where $f(v,t) = \partial F(v,t)/\partial v$ is the density function.

It has been shown that a similarity transformation $v^n t$ exists for Equation (1) provided a power law model holds for the transitional breakage probability, that is, $\Gamma(v) = kv^n$, and similar breakage, that is, $G(v,v') = g(v/v')$ (Fillipov, 1962; Ramkrishna, 1974). Ramkrishna (1974) applied the above similarity criteria to data on drop size distributions by Madden and McCoy (1969) and observed that the data were consistent with a power law model for the transition probability. In the present paper, we generalize the concept of similarity by assuming that droplets break in such a way that the daughter droplet size distribution function is

$$G(v,v') = g\left(\frac{\Gamma(v)}{\Gamma(v')}\right) \tag{2}$$

This is in contrast with the earlier concept of similar breakage which required that $G(v,v') = g(v/v')$. In either case, however, $g(x)$ is a distribution function for x between 0 and 1, since $\Gamma(v)$ is a monotone increasing function. It is interesting to note that the form (2) has distinct advantages over the form $g(v/v')$. To understand them, consider some sample breakage situations and how these situations are represented by the $G(v,v')$ which is the volume fraction of drops (formed by breakage of a parent drop of volume v') with volume between 0 and v. Figure 1 shows the shapes of $G(v,v')$ for three different situations of breakage. Case

I depicts what may be referred to as erosive breakage for which the volume fraction of daughter droplets would not ascent until v/v' is significantly greater than 1/2. Case II shows a thorough breakage, where the drop has been broken into several small droplets. For this case, the volume fraction must rise for v/v' substantially less than 1/2. Case III is binary equal (or approximately equal) breakage for which the volume fraction can be readily seen to possess the trend shown. It is significant to notice that for a given $x \equiv v/v'$, the volume fraction for case II is always more than that for case III. Little is known about how droplets in a turbulent, liquid-liquid dispersion break. Indeed, the papers of Acrivos and co-workers (1973, 1978, 1979) show that breakage of drops even in well-defined laminar flow situations can be a very complicated phenomenon. It seems reasonable to surmise, however, that larger droplets break somewhat as in case II (in Figure 1), while smaller droplets break more as in case III. Thus, a plot of

$$\tilde{G}(x;v') \equiv G(v,v'), \quad x \equiv \frac{v}{v'} \tag{3}$$

vs. x may be expected to shift to the left as v' increases. This implies that $[\partial \tilde{G}(x;v')/\partial v']_x$ must be positive valued. The earlier similarity form $g(v/v')$ implies that the foregoing derivative is identically zero, which forbids larger drops breaking more thoroughly than smaller drops. Thus, similarity as implied earlier is somewhat unrealistic.

Consider now the similarity form (2). The problem is to examine whether this form could admit the shifting of the curves of $\tilde{G}(v;v')$ vs. x to the left as v' increases. Now

$$\tilde{G}(x;v') = g\left[\frac{\Gamma(v'x)}{\Gamma(v')}\right] \tag{4}$$

so that

$$\frac{\partial}{\partial v'}\tilde{G}(x;v') = g'\left[\frac{\Gamma(v'x)}{\Gamma(v')}\right]\frac{1}{\Gamma(v')^2}[x\Gamma'(v'x)\,\Gamma(v') - \Gamma(v'x)\,\Gamma'(v')] \tag{5}$$

Since g is monotone, increasing g' is positive and the sign of the left-hand size of (5) is positive if and only if

$$x\Gamma'(v'x)\,\Gamma(v') - \Gamma(v'x)\Gamma'(v') > 0 \tag{6}$$

or

$$\frac{d\ln\,\Gamma(v'')}{d\ln\,v''} > \frac{d\ln\,\Gamma(v')}{d\ln\,v'} \quad (v'' < v') \tag{7}$$

Inequality (7) implies that a plot of $\ln\,\Gamma(v)$ vs. $\ln v$ must show an increasing slope as $\ln v$ decreases. Clearly, a power law model implies a constant value of $d\ln\,\Gamma(v)/d\,\ln v$, and the strict inequality (7) cannot be satisfied. Thus, if the transition probability function $\Gamma(v)$ is concave downward, then the form (4) can account for the postulated shift towards the left with increasing v' of the curves of $\tilde{G}(x;v')$ vs. x.* The similarity form (4) therefore presents a physically more plausible alternative to the form $g(v/v')$. An important advantage to the form (4) is that it admits the similarity transformation below.

Let $z = \Gamma(v)t$, $f(z) \equiv F(v,t)$. Substitution into Equation (1) yields the integral equation

$$\phi(z) = \int_z^\infty g\left(\frac{z}{\zeta}\right)\phi(\zeta)d\zeta \tag{8}$$

where $zf'(z) \equiv \phi(z)$. Whether or not the experimental data are consistent with the above concept of similarity requires a testing procedure, which is considered next.

Test for Similarity

Transients of drop volume distribution in a batch agitated lean liquid-liquid dispersion could be used to test for similar breakage as given by Equation (4).

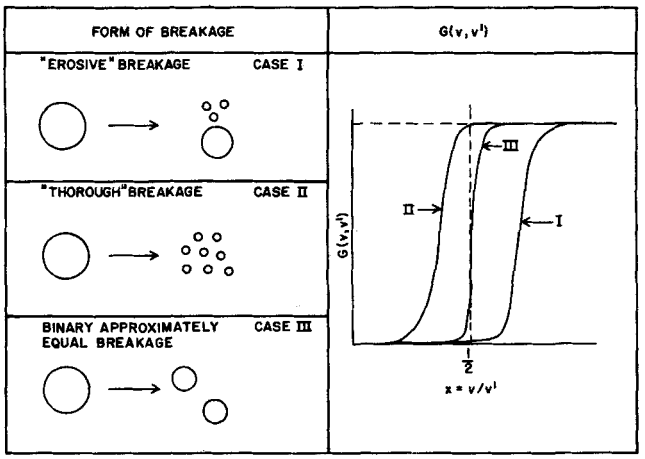

Figure 1. Daughter droplet distribution for different forms of breakage.

The experimental information consists of the cumulative drop volume distributions $F(v,t)$ at various times. For a fixed value of $F(v,t)$, v and t would be related by $\Gamma(v)t$ = constant (since the similarity variable must be constant at constant F). Thus

$$t\frac{d\Gamma(v)}{dv} + \left(\frac{\partial t}{\partial v}\right)_F \Gamma(v) = 0 \tag{9}$$

or

$$\frac{d\ln\Gamma(v)}{dv} + \left(\frac{\partial \ln t}{\partial v}\right)_F = 0 \tag{10}$$

Multiplying Equation (10) by v, one gets

$$\frac{d\ln\Gamma(v)}{d\ln v} = -\left(\frac{\partial \ln t}{\partial \ln v}\right)_F \tag{11}$$

Since the left-hand side of Equation (11) is independent of F, it provides a test of the similarity hypothesis. Experimental data on $F(v,t)$ can then be analyzed by plotting $\ln t$ vs. $\ln v$, holding F constant at various values. The slopes of such curves at any particular v must be independent of F. Thus, by a simple translation, the plots of $\ln t$ vs. $\ln v$ for different F's may be collapsed into a single curve from which $\partial \ln t/\partial \ln v$ may be estimated at various values of v. Integrating (11) from some convenient reference drop volume v_0 to v, we get

$$\Gamma(v) = \Gamma(v_0)\exp\left[-\int_{\ln v_0}^{\ln v}\left(\frac{\partial \ln t}{\partial \ln v}\right)_F d\ln v\right] \tag{12}$$

Clearly, the power law case is trivially accommodated by Equation (12), since it occurs when

$$-\left(\frac{\partial \ln t}{\partial \ln v}\right)_F = \alpha \tag{13}$$

where α is the exponent in the power law expression. For arbitrary forms of $\Gamma(v)$, Equation (12) can be integrated numerically from the data.

Once confirmation of the similarity concept has been made, the data on $f(v,t)$ can be collapsed into a single curve. However, Equation (12) determines only $\Gamma(v)/\Gamma(v_0)$ but not the required function $\Gamma(v)$. Obviously, the transformation $\Gamma(v)t/\Gamma(v_0) \equiv z'$ is also an admissible similarity variable, and we may collapse the entire data $F(v,t)$ into a single curve, say $\tilde{f}(z')$. The integral equation, which corresponds to (8), based on the similarity variable z' is given by

$$\tilde{\phi}(z') = \Gamma(v_0)\int_{z'}^\infty g\left(\frac{z}{\zeta'}\right)\tilde{\phi}(\zeta')d\zeta' \tag{14}$$

where $\tilde{\phi}(z') \equiv z'\tilde{f}'(z')$. We define moments

$$\tilde{\mu}_n \equiv \int_0^\infty (z')^n \tilde{f}(z')dz' \quad n = 1,2,\ldots \tag{15}$$

*It is interesting to note that the probabilistic model for transitional breakage probability $\Gamma(v)$ (Narsimhan et al., 1979) shows this trend.

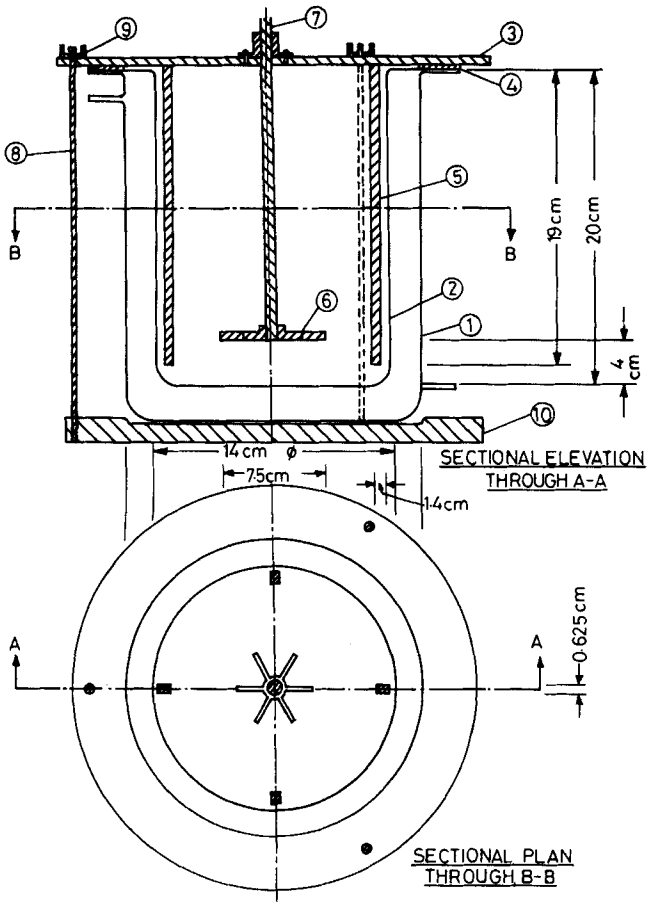

Figure 2. Plan and elevation of mixing vessel assembly.

1. Outer jacket
2. Vessel
3. Stainless steel plate of the baffle assembly
4. Rubber gasket
5. Baffle
6. Paddle impeller
7. Agitator shaft
8. Brass rod
9. Brass flynut
10. Bottom Aluminum plate

which can be computed from the similarity plot of $\tilde{f}(z')$ vs. z'. Also, we define constants

$$\nu_n \equiv \int_0^1 x^n\, g(x)dx \quad n = 0,1,2,... \tag{16}$$

Multiplying the integral Equation (14) by $(z')^{n-1}$, and integrating over $z' = 0$ to ∞, we find

$$\tilde{\mu}_n = \Gamma(v_0)\, \tilde{\mu}_{n+1}\, \nu_{n-1} \tag{17}$$

or

$$\Gamma(v_0)\nu_{n-1} = \frac{\tilde{\mu}_n}{\tilde{\mu}_{n+1}} \quad n = 1,2... \tag{18}$$

Details of this procedure are given elsewhere (Ramkrishna, 1974).

In principle, it should be possible to evaluate $\Gamma(v_0)\, g\,(x)$ from the moments $\{\Gamma(v_0)\nu_n\}$ as given by Equation (18) through a suitable polynomial expansion (Ramkrishna, 1973, 1974). Since $g(1) = 1$, it is clear that $\Gamma(v_0)$ is obtained from the evaluation of $\Gamma(v_0)g(x)$ at $x = 1$. However, since $g(x)$ is a cumulative daughter droplet volume distribution, it is only expected that the higher moments of $\Gamma(v_0)g(x)$ are important in the evaluation of $\Gamma(v_0)g(x)$. Though the moments $\{\Gamma(v_0)\nu_n\}$ progressively decrease as $g(x)$ is defined in the unit interval, they would probably not decrease fast enough to justify neglecting the higher moments in the evaluation of $\Gamma(v_0)g(x)$ through polynomial expansion. Moreover, evaluation of the moments of $\Gamma(v_0)g(x)$ would require knowledge of the moments of drop volume distribution of two orders greater, as can be seen from Equation (18). Since considerable errors would be involved in the evaluation of higher moments of drop volume distribution, it may not be possible to evaluate the higher moments of $\Gamma(v_0)g(x)$ accurately.

EXPERIMENTAL DETAILS

The transients of drop volume distribution in an agitated lean liquid-liquid dispersion were measured for three different dispersed phases, namely, CCl_4 *i*-octane mixture (50-50%), Anisole CCl_4 mixture (80-20%) and chlorobenzene. In all the experiments, the continuous phase was distilled water presaturated with the dispersed phase. The density and viscosity of both the phases were more or less equal. In fact, this dictated the choice of the dispersed phases.

Experiments were conducted in a 3l jacketed vessel, 0.14m in diameter, 0.20 m high. It was filled with the liquid-liquid mixture to a height of 0.1625 m. The outer jacket was provided for water circulation from a constant temperature bath in order to maintain constant temperature. All experiments were conducted at 30° ± 0.1°C. A six-blade ordinary paddle impeller of 0.0762 m diameter was used. The impeller was 0.009525 m wide and 0.00159 m thick. The impeller was placed at 0.04 m from the bottom of the vessel. Four stainless steel baffles 0.19 m long, 0.014 m wide and 0.625×10^{-2}m thick were equally spaced at 90 deg right angled to the vessel and 0.00635 m away from the wall. The details of the mixing vessel assembly are given in Figure 2. The agitator was driven by a 186.425 W induction motor with a variable speed drive. Experimental measurements were made at three agitator speeds, 480, 420 and 300 rev/min.

The droplets were encapsulated with a thin nylon film at the time of measurement through an interfacial polycondensation reaction. The encapsulation stops further breakage and coalescence of drops, thus freezing the population at the time of measurement. The reactants for the interfacial polycondensation reaction were terephthalic acid chloride and piperazine (Mylnek and Resnick, 1972). Terephthalic acid chloride was present in the dispersed phase at a concentration of 1% by weight. At the time of encapsulation, a mixture of piperazine and sodium hydroxide solutions were added to the continuous phase for the reaction to occur. The reaction was found to be instantaneous, resulting in a coating of very thin (0.1 to 1.0 μ) nylon film over all the droplets. The

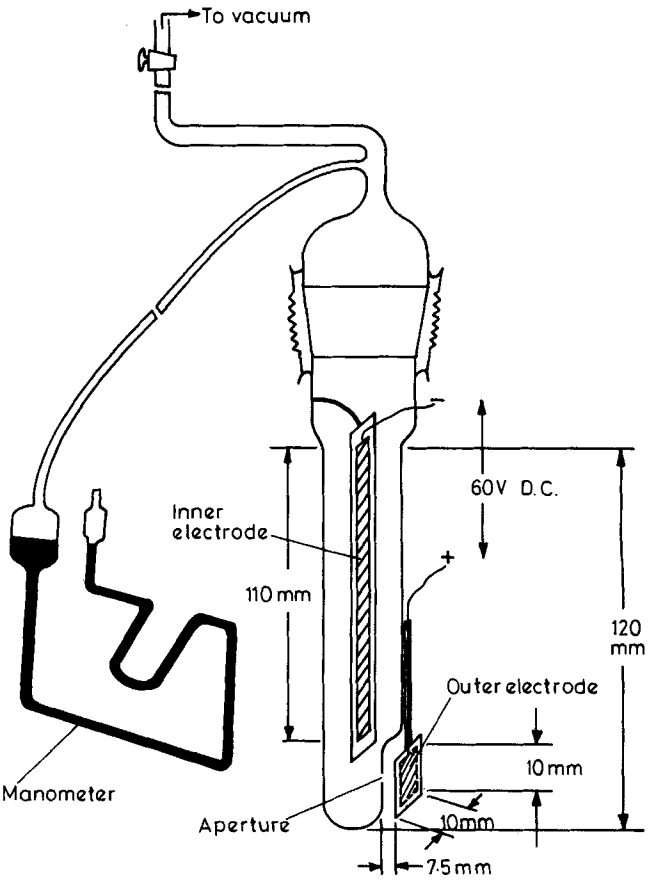

Figure 3. A schematic diagram of the probe assembly.

TABLE 1. SYSTEMS AND EXPERIMENTAL CONDITIONS

System	Agitator speed, rev/min
Water—CCl_4 + *i*-octane (50-50%)	480, 420, 300
Water—anisole + CCl_4 (80-20%)	300
Water—chlorobenzene	300

TABLE 2. PHYSICAL PROPERTIES OF DISPERSED PHASE

Dispersed phase	Density, kg/m³	Interfacial tension, N/m
CCl_4 + *i*-octane (50-50%)	114.9	46×10^{-3}
Anisole + CCl_4 (80-20%)	111.3	29×10^{-3}
Chlorobenzene	110.1	37.7×10^{-3}

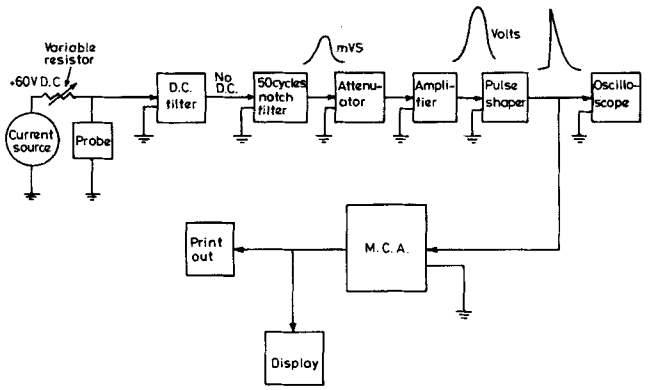

Figure 4. Block diagram of the electronic circuitory.

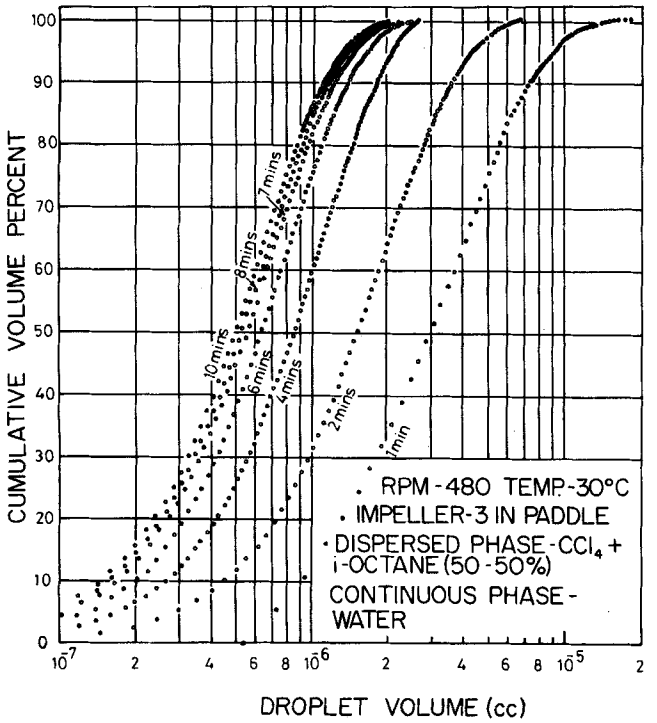

Figure 5. Effect of stirring time on drop volume distribution.

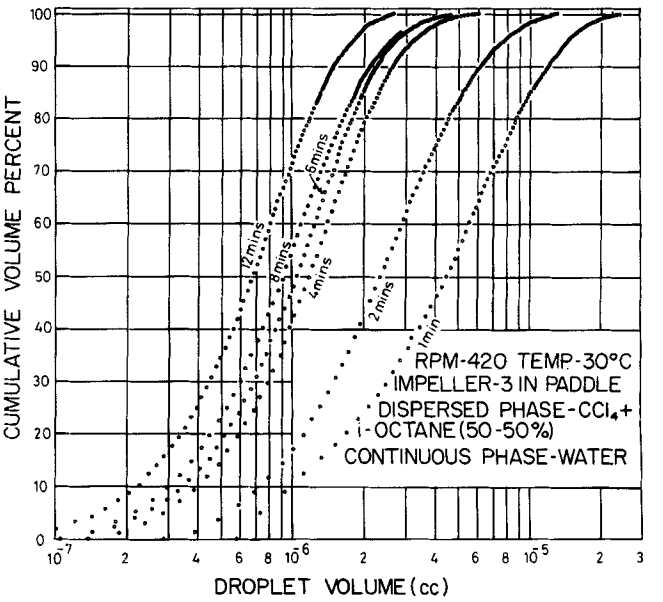

Figure 6. Effect of stirring time on drop volume distribution.

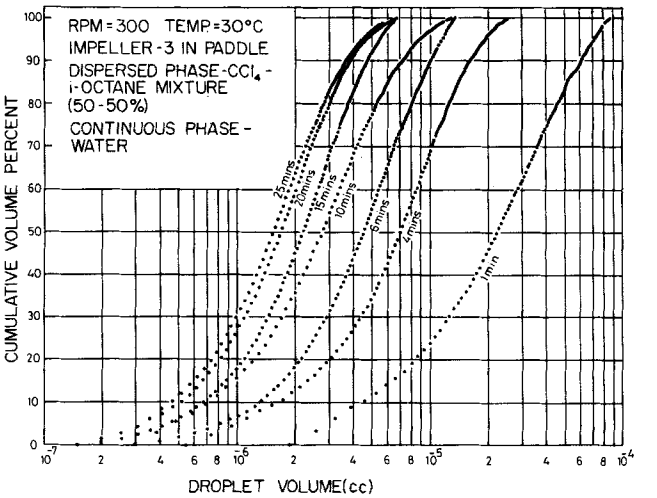

Figure 7. Effect of stirring time on drop volume distribution.

nylon film, being very thin, did not affect the drop volume measurement.

The volume distribution of encapsulated droplets was measured using electronic size analysis (Coulter counter). The suspension of encapsulated droplets was forced to flow through a small aperture having an immersed electrode on each side. As each encapsulated droplet passed through the aperture, it replaced an equivalent volume of the continuous phase, momentarily changing the resistance value between the electrodes. Since a constant current was maintained between the electrodes, this momentary change in the resistance value produced a voltage pulse of short duration having a magnitude proportional to the drop volume (Berg, 1966; Allen, 1959). The voltage pulses were amplified, scaled and counted to yield drop volume distribution.

Two glass probes of aperture diameters 2×10^{-3}m and 0.8×10^{-3}m were used. The schematic diagram of the probe assembly is shown in Figure 3. Probe consisted of a glass tube 0.015 m diameter fitted with a B-24 female joint, the flattened bottom portion of the tube having an aperture of required diameter. Platinum electrodes were used. Electrodes were made by embedding 2.54×10^{-5}m thick platinum foil on a glass plate. The inner electrode ran all along the length of the tube. The outer electrode faced the aperture with a gap of 7.5×10^{-3}m. Both the electrodes were kept rigid by connecting the glass plates carrying the electrodes to the tube. The dimensions of the inner and outer electrodes were 0.115×0.01 and 0.01×0.01 m, respectively. Here, the distance between the electrodes remained fixed since both the electrodes were embedded on glass plates.

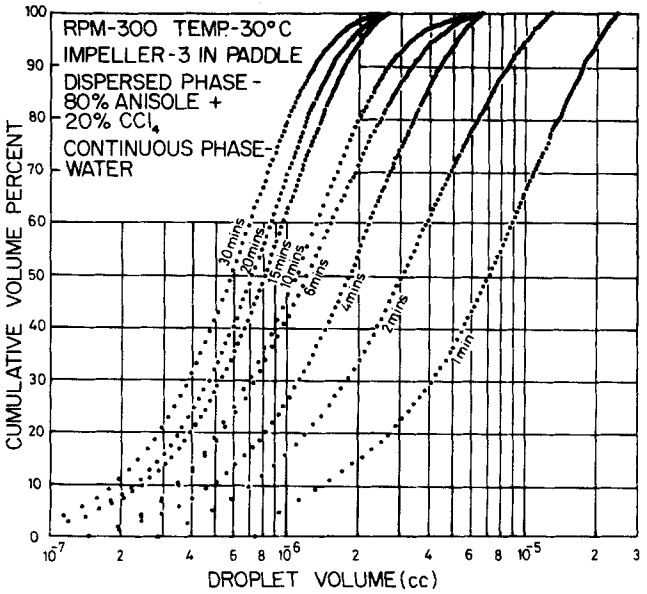

Figure 8. Effect of stirring time on drop volume distribution.

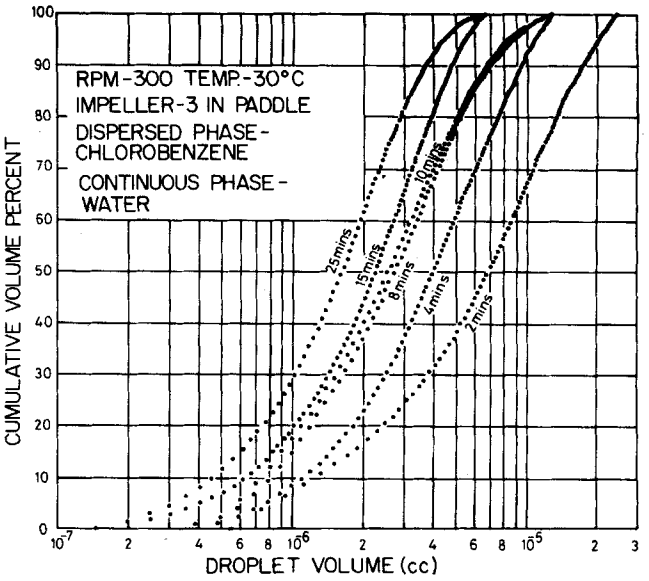

Figure 9. Effect of stirring time on drop volume distribution.

The probe tube was connected to a vacuum pump through a stopcock. The probe assembly was immersed in the suspending electrolytic medium, and the inner tube was filled with the medium. At the time of measurement, suction was applied to the tube by means of the vacuum pump, and the sample was withdrawn through the small aperture by opening the stopcock. The manometer connected to the probe gave the pressure drop across the aperture during suction.

The block diagram of the electronic circuitry is shown in Figure 4. The details of the circuitory can be found elsewhere (Narsimhan, 1979).

The amplitude of the voltage pulse given by a particle of certain volume will depend on many factors, such as aperture diameter, current, gain and attenuator settings and the resistance between the two electrodes. The relationship between the pulse amplitude and particle volume should be known in order to infer the droplet volume distribution from the output of Multichannel Analyser (MCA).

A narrow distribution of spherical standard sized glass particles were suspended in a conducting medium of sodium chloride solution. A sample of the suspended particles was withdrawn through the probe and the spectrum measured by the MCA. The average volume of the narrow sized standard sample was measured by microscopic counting. Since the sample is a narrow distribution of particles, the average particle volume should correspond to the average channel number of the spectrum. The same procedure was repeated for different sodium chloride concentrations, electronic settings and sample size to obtain the relationship between particle volume and channel number for different conditions. The details of the calibration are given elsewhere (Narsimhan, 1979).

Sometimes, more than one droplet may pass through the aperture simultaneously. This will give rise to the superimposition of the voltage pulses of these droplets, resulting in loss of count.

Coincidence corrections were checked experimentally by measuring the spectrum of standard sized spherical glass particles of narrow distribution at different concentrations in the size range of 50 to 800 μ. Since drop volume distribution measurements were made at dispersed phase volume fraction of 0.1%, coincidence effects were verified in the concentration range of 0.05 to 0.5%. It was found that the average channel number corresponding to the standard sample did not vary appreciably with concentration, indicating that the coincidence effects are negligible.

The mixing vessel, the stainless steel baffle assembly and the agitator were cleaned with chromic acid and rinsed thoroughly with distilled water. The mixing vessel was placed on the bottom aluminum plate. The baffle assembly was centered in the vessel and rigidly fixed by tightening the brass flynuts. The agitator was connected to the variable speed drive. The height of the impeller above the vessel bottom was checked. The probe assembly was lowered into the vessel through a hole provided in the top stainless steel plate so that the aperture of the probe was placed between two baffles and at half the depth of the vessel. The vessel was then charged with 2.5×10^{-3}m^3 of distilled water presaturated with the dispersed phase. Presaturation was done to avoid mass transfer of the dispersed phase into continuous phase during agitation. Water was circulated in the outer jacket of the vessel from a thermostat. The system was allowed to equilibrate for about ½ hr, after which it was found that the continuous phase temperature reached the set point in the thermostat. The continuous phase temperature was measured with a thermistor probe using a telethermometer. All experimental measurements were made at 30 ± 0.1°C.

One percent by weight of terephthalic acid chloride was dissolved in the dispersed phase. 2.5×10^{-6} m^3 of this was added to the continuous phase maintaining a dispersed phase volume fraction of 0.1%. The induction motor was started, and the time of agitation was measured with a stopwatch. The speed of agitation was checked for every observation with General Radio Strobotac. At the time of measurement, 5×10^{-5} m^3 of mixture of piperazine and sodium hydroxide was added to the continuous phase, and stirring continued for 10 s after which the speed of agitation was reduced. The dispersion was agitated at lower speed for a few minutes for the interfacial polycondensation reaction to be completed in order to increase the strength of nylon coating. Because of the presence of sodium hydroxide and formation of sodium chloride in polycondensation reaction, the continuous phase became a conducting medium. Vacuum was applied to the probe assembly through the vacuum pump. The stopcock in the outlet of the probe tube was then slowly opened to fill the probe with the dispersion. The resistance between the electrodes was then measured with a multimeter. The current, gain and attenuator settings were adjusted. Accordingly, the resistance of the series variable resistor was also adjusted. Electrophoresis power supply was put on to apply 60 V DC between the electrodes through the constant current source. The output from the amplifier was observed in the Phillips oscilloscope. Now, a sample of the dispersion was withdrawn through the aperture by slowly opening the stopcock at the outlet of the probe. The pressure drop across the aperture was checked with the mercury manometer connected to the probe. The pressure drop was adjusted by adjusting the opening of the stopcock. Same pressure drop was maintained during sampling for all observations. This was done to ensure that enough vacuum was applied to withdraw large size droplets. The amplified voltage pulse signals could be observed in the oscilloscope. The voltage range of the pulses was noted. If the pulses were not in the proper range (either too small or too big), then the current, attenuator and gain settings were adjusted accordingly so as to get the pulses in the proper range. The output from the pulse shaper was observed in the oscilloscope. If found satisfactory, it was fed to the MCA, and the pulses were logged in the MCA in PHA‡ mode. Usually, a sample of 2×10^{-4}m^3 was withdrawn at a time. Then the spectrum was observed in the visual display of the MCA. If the total number count of the droplets was not sufficient, then the withdrawn sample was recycled to the vessel and another sample of 2×10^{-4}m^3 was withdrawn, pulses logged in MCA. Around 10 000 droplets were counted to obtain a volume distribution. The printout of the spectrum was then taken. The same procedure was repeated to get another reading of the volume distribution. This was done to check the consistency of the measured distribution. The voltage drop between the electrodes was then measured with the multimeter.

The different systems and experimental conditions are given in Table 1. The physical properties of the dispersed phases are given in Table 2. The interfacial tension measurements were made at 30°±0.1°C by drop

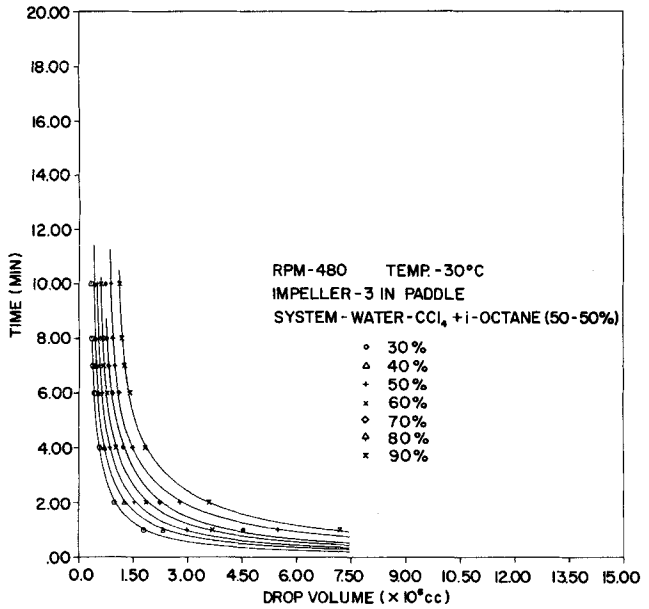

Figure 10. Plot of stirring time vs. drop volume for a fixed cumulative volume percent.

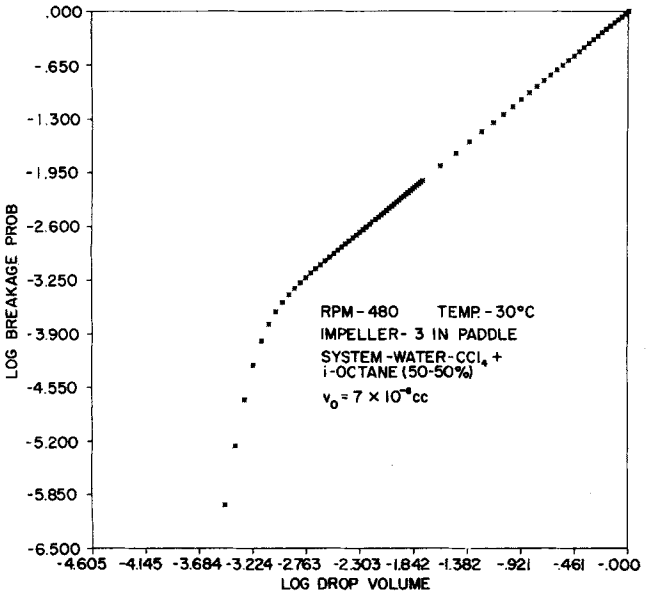

Figure 12. Plot of $\Gamma(v)/\Gamma(v_0)$ vs. v/v_0.

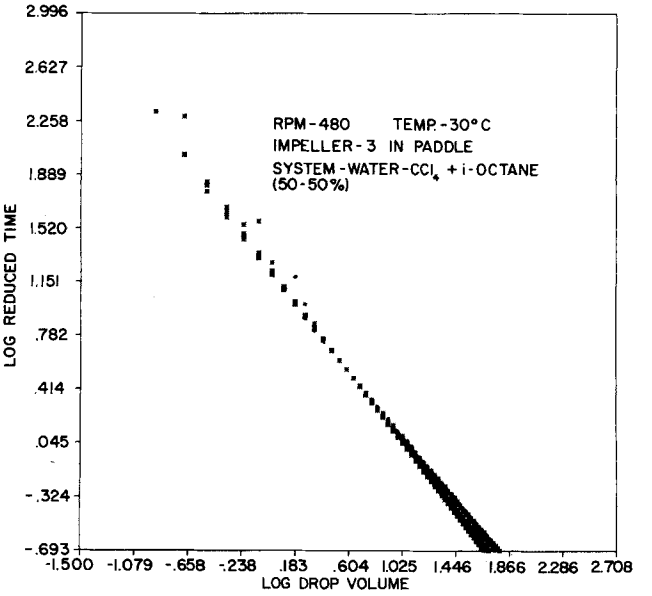

Figure 11. Plot of reduced time vs. drop volume.

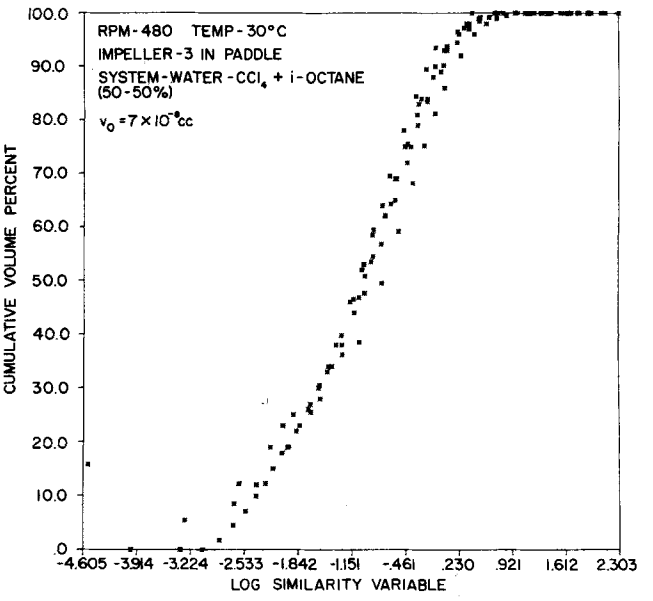

Figure 13. Plot of cumulative volume percent vs. similarity variable $\Gamma(v)\cdot t/\Gamma(v_0)$.

weight method. Most of the experiments were conducted at the dispersed phase fraction of 0.1%. Measurements were also made at three more dispersed phase volume fractions, namely, 0.25, 0.375 and 0.5%, to study the effect of dispersed phase fraction on drop volume distribution. The dispersed phase fraction was found to have negligible effect on drop volume distribution, thus indicating that coalescence was negligible. The reproducibility of measurement was tested employing Kolmogorov-Smirnov two sample tests which showed that the experiments were reproducible (Narsimhan, 1979).

Figures 5 through 9 give the effect of stirring time on drop volume distribution for the above measurements.

TEST OF EXPERIMENTAL DATA FOR SIMILARITY

Figure 10 gives a typical plot of stirring time vs. drop volume for different fixed cumulative volume percents. The solid curves in the figure indicate the curves fitted to the experimental data through least squares.*

*Figure 10 is representative of similar plots which were obtained for all the systems and experimental conditions in this work. They are not presented here for conciseness of presentation. These observations also hold for Figures 11 and 12.

‡PHA = Pulse Height Analysis.

From Equation (11), we see that $(\partial \ln t/\partial v)$ should be independent of cumulative volume percent if similarity holds. The curves of stirring time vs. drop volume are labeled as $1,2,3 \ldots n$ corresponding to cumulative volume percents F_1, F_2, $\ldots$ F_n, etc. A large number (around 200) of drop volumes $v_1, v_2, \ldots v_m$ are chosen. The coefficient of variation of $(\partial \ln t/\partial v)$ at v_k is given by

$$\epsilon^k = \frac{\frac{1}{\frac{n}{2}}\left(\sum_{i=1}^{n}\sum_{j\neq i}^{n}\alpha_{ij}{}^{k}\right)^{1/2}}{\frac{1}{n}\sum_{i=1}^{n}\beta_i^k} \qquad (19)$$

where

$$\alpha_{ij}{}^{k} = \left[\left(\frac{\partial \ln t}{\partial v}\right)_{F_i} - \left(\frac{\partial \ln t}{\partial v}\right)_{F_j}\right]^2_{v=v_k} \quad \text{and} \quad \beta_i{}^{k} = \left(\frac{\partial \ln t}{\partial v}\right)_{v=v_k, F_i}$$

A reference drop volume v_l is chosen such that ϵ^l is minimum.

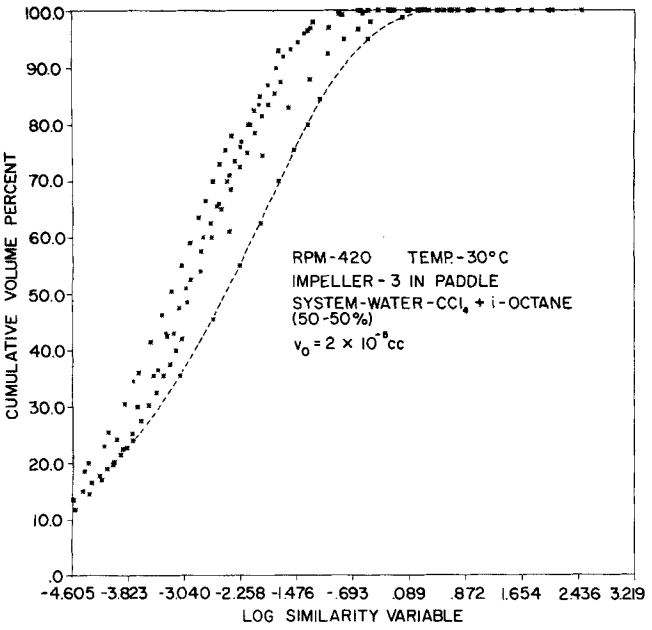

Figure 14. Plot of cumulative volume percent vs. similarity variable $\Gamma(v)\cdot t/\Gamma(v_0)$.

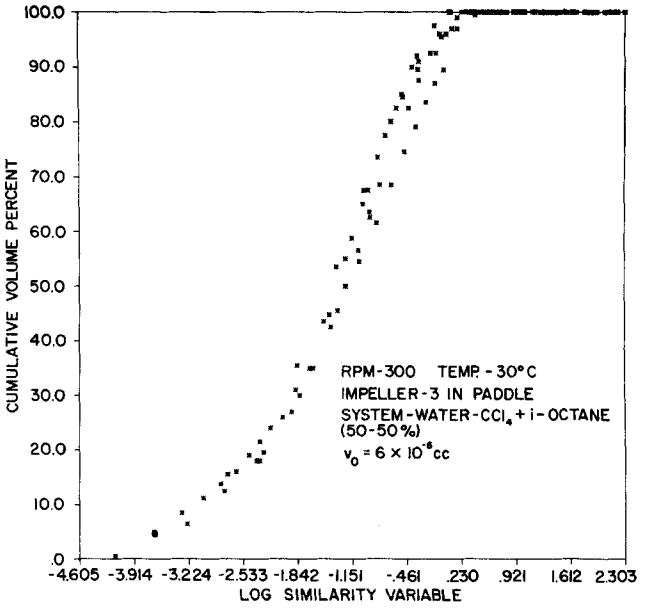

Figure 15. Plot of cumulative volume percent vs. similarity variable $\Gamma(v)\cdot t/\Gamma(v_0)$.

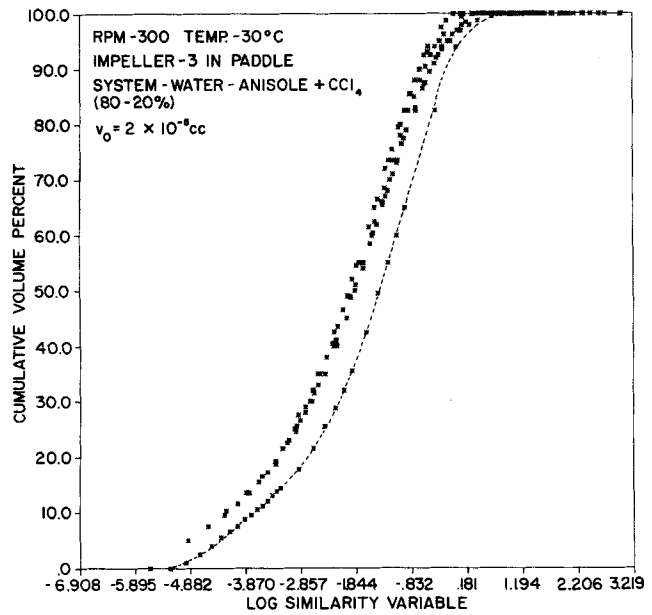

Figure 16. Plot of cumulative volume percent vs. similarity variable $\Gamma(v)\cdot t/\Gamma(v_0)$.

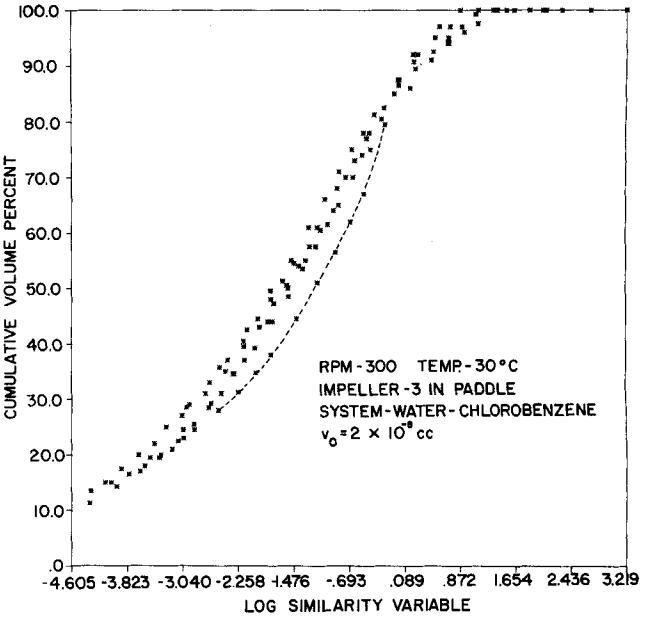

Figure 17. Plot of cumulative volume percent vs. similarity variable $\Gamma(v)\cdot t/\Gamma(v_0)$.

ln$t$ *vs.* v curves are translated along the ordinate with respect to a reference cumulative volume percent (The reference is 50% cumulative volume percent in all the cases.)
The translation factor γ_i is given by

$$\gamma_i = \ln\left(\frac{t_r}{t_i}\right)$$

t_r and t_i being the times at the reference drop volume v_l.

Figure 11 gives a typical plot of ln$t$ vs. ln$v$ after the translation of all points corresponding to $\{v_i\}$, $i=1,2,3, \ldots m$ along the ordinate. The points collapse into a single curve, thus justifying the similarity hypothesis. The scatter is found to be more for the low agitator speed of 300 rev/min for all the three systems. The scatter seems to be more pronounced at low droplet volumes. Stirring time vs. droplet volume curves rise steeply at very low droplet volumes as can be seen from Figure 10. This is to be expected, as the rate of breakage decreases rapidly with decrease in drop volume. The curves for different cumulative volume percents do not approach the same asymptote, contrary to expectation. This may be due to experimental errors at very low drop volumes. More scatter in the collapsed curves at low drop volumes may be attributed to this experimental error.

The transitional breakage probability $\Gamma(v)$ is estimated with reference to a reference drop volume through integration of the collapsed curve as given by Equation (12). Figure 12 gives a typical plot of estimated $\Gamma(v)/\Gamma(v_0)$. It is very interesting to note that the estimated transitional breakage probability does not satisfy a power law expression. The shape of the estimated $\Gamma(v)/\Gamma(v_0)$ seems to agree well with the probabilistic model for transitional breakage probability. Moreover, the estimated $\Gamma(v)/\Gamma(v_0)$ could be approximated by two power law expressions for different drop volume regions and the value of the exponent increases as the drop volume decreases, which is consistent with

TABLE 3. MOMENTS OF $\Gamma(v_0)\, g(x)$

System	Agitator speed, rev/min	v_0 ($\times 10^{12}$ m^3)	ν_0	ν_1	ν_2	ν_3
Water—CCl_4 + *i*-octane (50-50%)	480	7	0.3343	0.1939	0.1520	0.1360
	420	20	0.3100	0.1415	0.1124	0.0996
	300	60	0.1187	0.0735	0.0595	0.0532
Water—anisole + CCl_4 (80-20%)	300	20	0.1554	0.0729	0.0541	0.0461
Water—chlorobenzene	300	20	0.1965	0.0684	0.0472	0.0428

TABLE 4. COMPARISON OF MOMENTS OF $\Gamma(v_0)\, g(x)$ FOR DIFFERENT REFERENCE DROP VOLUMES [REV/MIN—480, WATER—CCl_4 + *i*-OCTANE (50-50%)]

v_0 ($\times 10^{12}$ m^3)	$\Gamma(v_{0r})/\Gamma(v_0)$	ν_n	ν_{nr}/ν_n
7.0	1.0	0.3343	1
		0.1939	1
		0.1520	1
		0.1360	1
10.0	0.6610	0.4933	0.6777
		0.3041	0.6374
		0.2375	0.6398
		0.2096	0.6487
12.4	0.515	0.6194	0.5396
		0.4018	0.4825
		0.3140	0.4840
		0.2733	0.4974

the behavior of the model for transitional breakage probability (Narsimhan et al., 1979). The behavior of estimated $\Gamma(v)/\Gamma(v_0)$ is consistent with the functional form of daughter droplet distribution for similar breakage. It is also found to be consistent with the concept of a maximum stable drop diameter. In fact, the maximum stable drop volumes could be estimated in case of water- ccl_4 + *i*-octane system at the three agitator speeds through extrapolation, as the estimated $\Gamma(v)/\Gamma(v_0)$ exhibits an appreciable drop with the decrease in drop volume at very low drop volumes. Such an attempt is desisted, as the estimation of $\Gamma(v)/\Gamma(v_0)$ at very low drop volume is only qualitative due to more scatter at low drop volumes resulting from experimental error.

The estimated transitional breakage probability function $\Gamma(v)/\Gamma(v_0)$ is used to transform the drop volume distributions $F(v,t)$ at different stirring times under the transformation $z' = \Gamma(v)\cdot t/\Gamma(v_0)$. Figures 13 through 17 give the plot of drop volume distributions with respect to the similarity variable $\Gamma(v)\cdot t/\Gamma(v_0)$. The drop volume distributions at different stirring times do collapse into a single curve, as can be seen from Figures 13 through 17. The agreement of similarity seems to be excellent for the water-ccl_4 + *i*-octane (50-50%) system at the agitator speeds of 480 and 300 rev/min. In the other three cases, all drop volume distribution curves except the distribution at very low stirring times collapse into a single curve. The distribution curves corresponding to low stirring times are indicated by dashed curves in Figures 14, 16 and 17. At very small stirring times, the drop volume distribution may not tend to a limit distribution and hence may not satisfy similarity (Fillipov, 1961). It may also be due to experimental errors involved in the measurement of large drop volumes. The inherent drawback of encapsulation technique is that the measurement of transients of drop volume distribution would necessitate repetition of experiments at identical conditions for different stirring times, as the drop population is frozen at the time of measurement. Therefore, a small difference in experimental conditions may result in large errors at very low stirring times, as drop breakage rate is very high for large drop volumes. Moreover, the accuracy of the measurement hinges mainly on the strength of the interfacial nylon film formed due to interfacial polycondensation reaction. It was found that the nylon film was stronger for small drop volumes, thus making large encapsulated drops more susceptible to breakage during sampling.

Moments of $\Gamma(v_0)g(x)$ were computed from the moments of $\tilde{f}(z')$ using Equation (18). Table 3 gives the first three moments of $\Gamma(v_0)\, g(x)$ for all the experimental conditions. Estimation of $\Gamma(v_0)$ and $g(x)$ from the moments through orthogonal polynomial expansion was desisted due to errors involved in such an estimation as mentioned earlier.

It is easily seen from Equations (15) and (18) that

$$\gamma_n = \frac{\Gamma(v_{02})}{\Gamma(v_{01})}\nu_n \tag{20}$$

where $\{\nu_n\}$ and $\{\gamma_n\}$ are the moments of $\Gamma(v_{01})g(x)$ and $\Gamma(v_{02})g(x)$, respectively. Since the reference drop volume v_0 in the estimation of transitional breakage probability is arbitrary, the consistency of the moments of $g(x)$ could be verified through Equation (20). Table 4 gives the first three moments of $\Gamma(v_0)g(x)$ for three different reference drop volumes for water − CCl_4 + *i*-octane (50-50%) system at the agitator speed of 480 rev/min. It can be seen from Table 4 that the ratios of the estimated moments for different reference drop volumes agree fairly well with the ratio of transitional breakage probabilities at reference volumes.

ACKNOWLEDGMENT

The authors wish to acknowledge the National Science Foundation for partial support of the work through NSF Research Grant ENG 77-19367.

NOTATION

f = drop volume density
F = cumulative drop volume distribution
g = cumulative daughter droplet distribution for "similar" breakage
G = cumulative daughter droplet distribution
t = time
v = drop volume
x = ratio of transitional breakage probabilities of daughter and parent droplets
z = similarity variable

Greek Letters

γ = translation factor; also used as moments of daughter droplet distribution
ϵ = coefficient of variation
Γ = transitional breakage probability
μ = moments of drop volume distribution
ν = moments of daughter droplet distribution

Subscripts

i = i^{th} curve
o = reference drop volume
n = n^{th} moment
nr = n^{th} moment with respect to the reference drop volume
r = reference curve

Superscripts

$\sim$ = modified similarity variable

LITERATURE CITED

Acrivos, A., and T. S. Lo, "Deformation and Breakup of a Single Slender Drop in an Extensional Flow," *J. Fluid Mech.*, **86**, 641 (1978).

Allen, T., *Particle Size Measurement*, Chapman and Hall, Ltd, MacMillan, New York (1959).

Barthe's - Biesel, D., and A. Acrivos, "Deformation and Burst of a Liquid Droplet Freely Suspended in a Linear Shear Field," *J. Fluid Mech.*, **61**, 1 (1973).

Berg, R. H., "Electronic Size Analysis of Sub-Sieve Particles by Flowing Through a Small Liquid-Resistor," Symposium on Particle Size Measurement, Sixty-First Annual Meeting Papers ASTM Special Technical Publication No. 234, p. 245 (1966).

Fillipov, A. F., "On the Distribution of the Sizes of Particles Which Undergo Splitting," *Theory Prob. Applic.*, **6**, 275 (1961).

Hinch, E. J., and A. Acrivos, "Steady Long Slender Droplets in Two-Dimensional Straining Motion," *J. Fluid Mech.*, **91**, 401 (1979).

Levich, V. G., Physicochemical Hydrodynamics, Prentice-Hall, Englewood Cliffs, N.J. (1972).

Madden, A. J., and B. J. McCoy, "Drop Size in Stirred Liquid-Liquid System Via Encapsulation," *Chem. Eng. Sci.*, **24**, 416 (1969).

Mlynek, Y., and W. Resnick, "Drop Sizes in an Agitated Liquid-Liquid System," *AIChE J.*, **18** 122 (1972).

Narsimhan, G., "Drop Breakage in Agitated Lean Liquid-Liquid Dispersions," Ph.D. dissertation, I. I. T. Kanpur, India (1979).

———, J. P. Gupta and D. Ramkrishna, "A Model for Transitional Breakage Probability of Droplets in Agitated Lean Liquid-Liquid Dispersions," *Chem. Eng. Sci.*, **34**, 257 (1979).

Ramkrishna, D., "On Problem Specific Polynomials," *Chem. Eng. Sci.*, **28**, 1362 (1973).

———, "Drop Breakage in Agitated Liquid-Liquid Dispersions," *ibid.*, **29**, 987 (1974).

Manuscript received October 1, 1979, and accepted January 23, 1980.

Photo-Assisted Heterogeneous Catalysis with Optical Fibers
II. Nonisothermal Single Fiber and Fiber Bundle

A previous paper (Marinangeli and Ollis, 1977) considered light transport in a single optical fiber which was coated with a heterogeneous photoassisted catalyst. This paper analyzes simultaneous mass, heat, and light transport in a catalyst on a single fiber, and in a likely large-scale configuration, a bundle of parallel, catalyst-coated optical fibers. The dimensionless temperature rise is dominated by energy released by light absorption, with the heat of reaction contributing to a lesser degree.

R. E. MARINANGELI

and

D. F. OLLIS

Dept. of Chemical Engineering
Princeton University
Princeton, NJ 08544

SCOPE

Photo-assisted catalysts are known to effect alkane partial oxidation, photo-electrolysis of water, and degradation of halogenated hydrocarbons, among other reactions. The potential for large-scale development of heterogeneous photo-assisted catalysis may likely require, *inter alia*, a large surface area per reactor volume for the transport of light to the catalyst surface. Our previous paper (Marinangeli and Ollis, 1977) suggested that catalyst-coated, small diameter optical fibers might satisfy such a criterion. This paper considers simultaneous transport of light, heat and reactant in two heterogeneous, photo-assisted catalyst configurations: the single coated fiber, and the bundle of parallel coated fibers.

Literature reports of quantum yields (molecules converted per photon absorbed) are usually 0.1 to 10%, and typical photon energies are of the order of a moderate heat of reaction. Consequently, for single fibers or fiber bundles, the dimensionless temperature rise is necessarily dominated by energy released on light absorption for all values of the Prater number. The approximate temperature independence of photochemical kinetics (below the temperature of catalyst deactivation) allows consecutive determination of concentration and temperature profiles. For catalysts which are inactive above temperature T^*, the dominant contribution of absorptive heating (unchanged by reaction) allows determination of the maximum useful bundle diameter for a given illumination intensity, or maximum intensity for a given bundle diameter. Transport limitations may lead to kinetics dominated either by slow mass diffusion or by insufficient local illumination.

This analysis applies to systems such as catalytic films of chloroplasts or other intact photosynthetic systems, metal complexes, or semiconductors. The special case of semiconductors which function as photoelectrodes when coated on optical fibers is analyzed in a subsequent paper (Marinangeli and Ollis, 1980).

Correspondence concerning this paper should be addressed to D. F. Ollis, Dept. of Chemical Engineering, Univ. of California, Davis, CA 95616.

R. E. Marinangeli is presently with Universal Oil Products, Des Plaines, Ill.

0001-1541-80-1000-9626-$01.05.